Brodogradnja/Shipbuilding/Open access Volume 68 Number 3, 2017

Nikola Matulić
Nikola Račić
Gojmir Radica

http://dx.doi.org/10.21278/brod68307 ISSN 0007-215X
eISSN 1845-5859

SUPERCHARGED ENGINE USING TURBINE STANDALONE EXHAUST GAS RECUPERATION SYSTEM

UDC 629.5.038
Original scientific paper

Summary

This paper presents a new hybrid concept that increases the overall efficiency of the propulsion system on ships. The hybrid concept of the marine propulsion system was examined in 1D CFD internal combustion engine model where the turbine and compressor are not mechanically connected. Such a configuration makes possible different turbine designs than needed in the conventional turbocharger. The advantage is an increased recuperation of energy from exhaust gases. By means of computer simulation and optimization, this study proves that the hybrid concept significantly increases the propulsion system efficiency and lower emissions in maritime environment.

Key words:

1. Introduction

This is perhaps the most exciting era in the history of the development of internal combustion engines, due to increasingly stricter international regulations *Hybrid engine; exhaust gas recuperation* on exhaust emissions and the requirements of users with regard to engine performance and reliability. Demands for propulsion system efficiency have fostered the progress of both the automobile industry, as the front-runner in the development of engine technologies, and the shipbuilding industry applying internal combustion engines for propulsion. Over the past decade, a number of new technologies have been introduced into both industries, e.g. direct fuel injection, turbo-charging and variable inlet and exhaust valve timing. The implementation of these technologies has considerably reduced the operating volume of modern engines (downsizing). The engine's operating points have been preserved within a more efficient operation range, thus reducing fuel consumption, increasing engine performance, and maintaining exhaust emissions within statutory limits. The constraints of the applied technologies include detonation in the cylinder occurring at higher turbocharging pressures, high compression ratios and pre-ignition. For instance, such constraints can be found in a design of the turbocharger with limited charging pressure that restricts potential recovery of the exhaust gas energy. In addition to the above technologies, the focus is on reduction in weight, friction and loss of working media when designing the engine and control strategies [1], [2]. The hybrid design also represents one of the essential technologies aimed at reducing fuel consumption and exhaust gas emissions [3]. The increase in efficiency of the low speed two-stroke turbocharged main compression ignition (CI) engine, operating with waste heat recovery through combined heat and power production, has been explored by researchers [4, 5], including the thermodynamic analysis of the IC engine for the purpose of diagnostics and optimisation [6]. Fu and others [7], in their research, explained the combined air cycle concept for IC engine supercharging, based on the exhaust gas energy recovery, which can effectively improve the efficiency of IC engines. The effect of EGR on NOx emission of methane is higher than in other fuels and its effect on IMEP of hydrogen is lower than in other fuels. From the viewpoint of emission and power, 10% of EGR seems to be the most desirable amount. The most noticeable effect of supercharging is with the gasoline system, while hydrogen concepts seem to be affected the least [8]. The supercharging system of the engine which is characterized by two turbochargers [9] showed that Air/Fuel ratio and low and high pressure compressor pressure ratios were the most influential parameters affecting engine output power and specific fuel consumption.

2. Turbine-engine recuperation system (TERS)

Due to relatively low efficiency of the internal combustion engines and, on the other hand, poor autonomy of otherwise very efficient electric-drive transport systems, investments have been increasingly placed in the development of hybrid arrangements where internal combustion engines are combined with battery and electric motor systems. In this area, particular attention is paid to the recuperation of the waste heat that is used to produce heat energy or mechanical work. This issue deserves careful consideration because, in internal combustion engines, about 50% of the energy produced by fuel is lost as waste heat. Exhaust gases alone contain 30% of the waste heat. Therefore, the heat energy contained in exhaust gases is particularly suitable to be recovered as energy for utility boiler operation or conversion into mechanical work by means of turbo-engines. Owing to the substantial development of batteries, the attention of this study has been focused on the concept of converting the waste heat energy contained in exhaust gases into mechanical work that drives generators to charge batteries.

The trend of enforcing restrictions on the harmful exhaust emissions from ships has encouraged engine manufacturers to seek alternative solutions. The concept presented in Figure 1 is one of the possible solutions for the forthcoming development of propulsion systems in smaller passenger vessels, patrol boats, workboats and yachts.

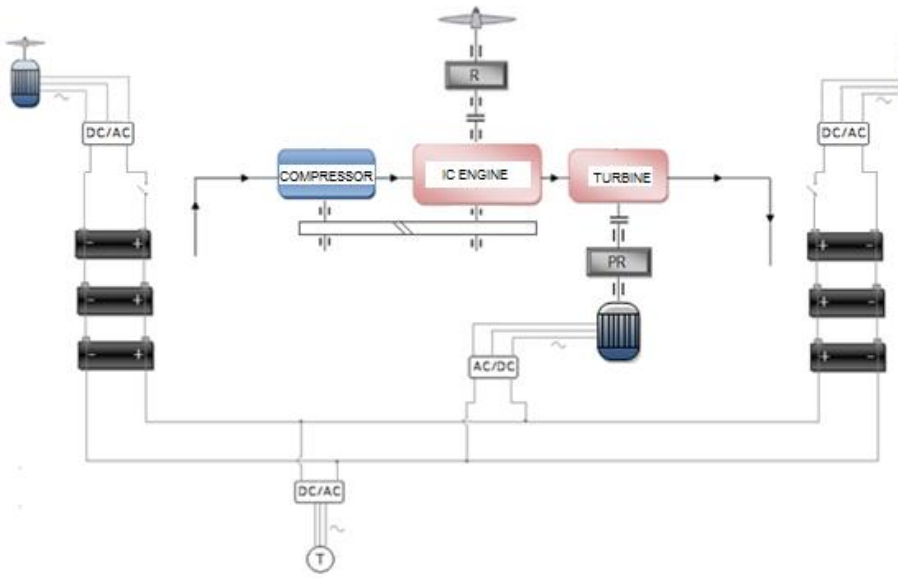

Fig. 1. Turbine-engine recuperation system (TERS)

The presented hybrid modular drive consists of an internal combustion engine, a compressor, a turbine, a set of lithium batteries fitted with rectifiers, two electric motors and a power transmission system. The concept features two modes of operation. The first mode of operation involves the internal combustion engine that runs during long passages, when the power is generated by the turbine and the engine itself. It should be noted that the turbine and the compressor are not mechanically connected, thereby allowing better efficiency of the turbine and increased energy recuperation from exhaust gases, which is not the case in turbo-chargers. Hence the internal combustion engine supplies energy to the compressor via the belt drive and the turbine conveys the energy to the generator.

In another mode of operation, the internal combustion engine is shut down and the central propeller shaft clutch is disconnected. The vessel is now driven exclusively by electric power supplied by lithium batteries. The control can be performed by turning the side screws or by using special electronic modules that regulate the power of each individual screw. In the mode of battery discharge, the switch before the DC/AC adapter is on.

The advantage of this hybrid propulsion, compared to conventional marine hybrid drives (Figure 2) fitted with a shaft generator on one main propeller shaft, is that the turbine makes use of energy which is stored in batteries, making a significant portion of their capacity. Maximum charging power is defined by maximum generator power, i.e. the maximum power recuperated by the turbine. Another advantage is a wider output range when selecting electric motors for this propulsion plant because power can be metered by the internal combustion engine.

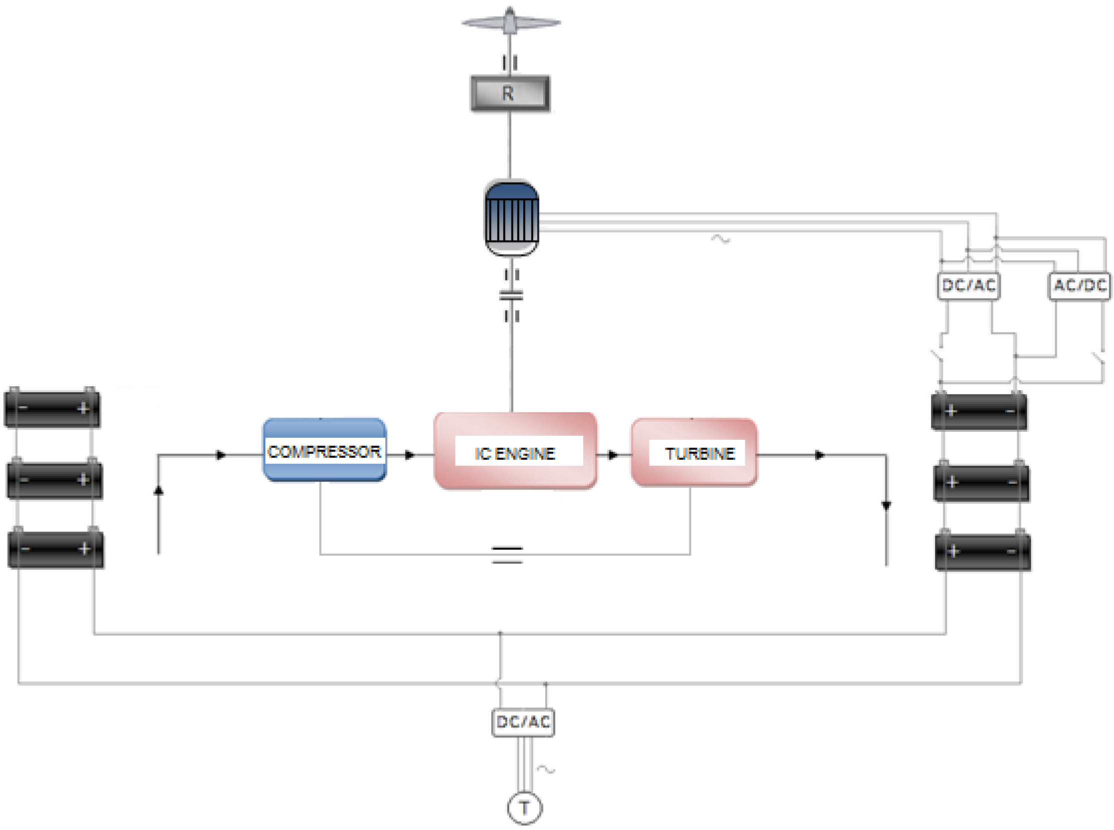

Fig. 2. Conventional hybrid system in the marine propulsion

There is a long tradition of using compression ignition (CI) engines in marine propulsion, but spark ignition (SI) engines appear to be more suitable for designing hybrid systems due to their high efficiency, low fuel consumption, low harmful gas emission, and the electronic regulation of the engine operation which becomes increasingly precise. Because of the complexity of such hybrid systems resulting from reliability and safety requirements, as well as because of high fuel prices, the application of these systems would be most cost-efficient in smaller vessels. These are the reasons for choosing a spark ignition (SI) engine for further analysis of the concept. The engine selection was carried out in line with the required power for the vessel's propulsion, which is defined by the admiralty equation. The single-chine V-hull is 12 meters in length on the waterline, with 6 ton displacement and the desired speed of 22 knots. The adequate propulsion for this hull and speed is 160 kW, which matches the naturally aspirated four stroke high speed engine with the swept volume of 4.3 litres and electronic injection in inlet ports to each of its 6 cylinders. The design and the analysis of the concept has been performed in a 1D simulation package intended exclusively for the simulation of processes in internal combustion engines. Initially, a naturally aspirated engine model was designed and calibrated according to manufacturer's specifications. It was then fitted with a turbine and a compressor. The objective was to maintain the engine's performance at reduced fuel consumption, i.e. to increase the system's efficiency by using the concept described in Figure 1.

3. Engine model

In order to analyse the concept, it is necessary to design a model for a naturally aspirated engine, making sure that it is calibrated in line with the performances declared by the manufacturer. The model for the inlet and exhaust gates is based on the 1D Navier-Stokes equation, the combustion is based on the single-zone model, while the heat transfer in the cylinder is defined by Woschni equation (Figure 3). The modelling and subsequent optimisation have been performed using Lotus software package.

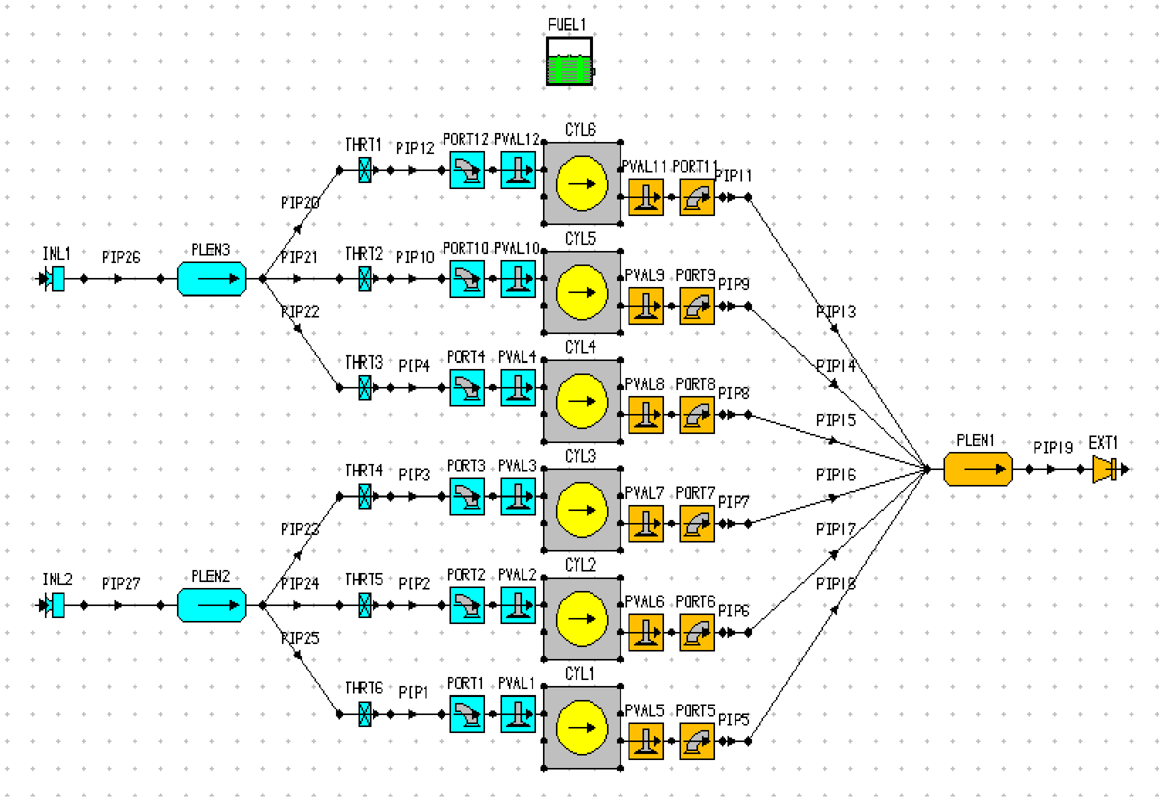

Fig. 3. Model of four stroke high speed 4.3l engine in Lotus

The Lotus software was used for modelling a naturally aspirated engine with six cylinders, two inlet manifolds, each serving three cylinders, and one exhaust collector. The 9.4 compression ratio is suitable for turbocharged engines, which comes in handy for further model upgrade with a turbo-compressor. Each cylinder houses four valves, two inlet and two exhaust valves. Load regulation is performed through butterfly flaps. Combustion is modelled using a single Vibe function with a coefficient *m*=2 over the equation (1).

$$m_{frac} = 1 - exp^{-A\left(\frac{\theta}{\theta_b}\right)^{M+1}} \qquad (1)$$

Where m_{frac} is the fraction of burned fuel mass, A and M are coefficients of the Vibe function, θ is the crankshaft angle and θ_b is the combustion period. The heat release profile is shown in Figure 4.

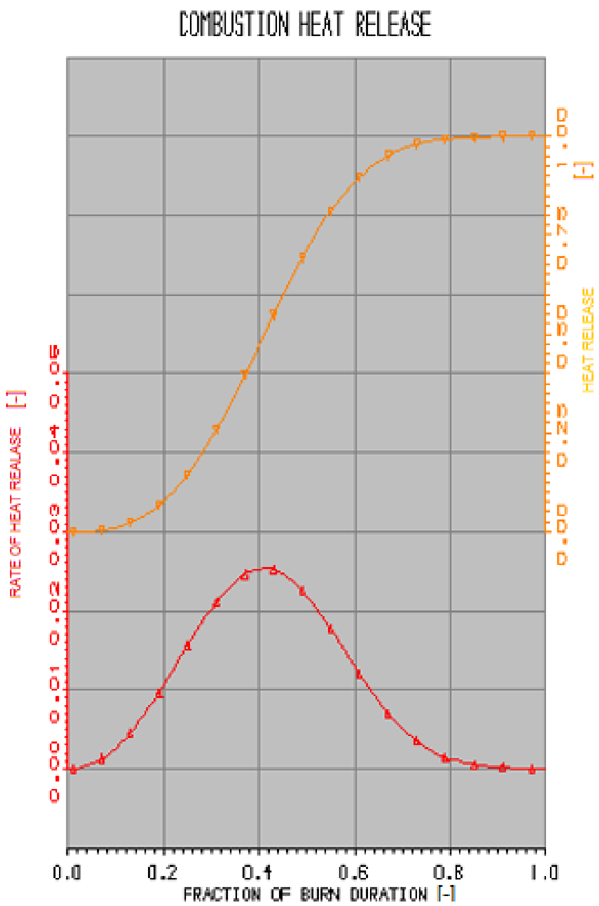

Fig. 4. Heat release for selected coefficients of the Vibe function

The combustion period (burn duration) is presented empirically by the expression [10]:

$$10 - 90\%\ (deg) = 20\left(\frac{\text{Bore}}{\text{Stroke}}\right) + 0.6\left(\frac{\text{Speed}\cdot\text{Stroke}}{30} - 11\right) \tag{3}$$

The convective heat transfer in the cylinder is modelled through the relation:

$$dQ = A \cdot h \cdot (T_{gas} - T_{wall}) \tag{4}$$

where the heat transfer coefficient h is defined by Woschni relation:

$$h = \frac{Ap^{0.8}}{T^{0.55} {D_{cyl}}^{0.2}}\left(B\bar{U}_{piston} + C\bar{U}_{swirl} + D\,\frac{T_{SOC}V(p - p_{motor})}{p_{SOC}V_{SOC}}\right)^{0.8} \tag{5}$$

where A, B, C and D are Woschni coefficients, p is the cylinder pressure, T cylinder temperature, V cylinder volume, $\bar{U}_{piston}$ mean piston speed, $\bar{U}_{swirl}$ mean swirl speed, T_{SOC} temperatures at the start of combustion, p_{SOC} pressure at the start of combustion, V_{SOC} volume at the start of combustion, and p_{motor} is the motoring pressure.

The swirl ratio is defined as:

$$\bar{U}_{swirl} = \frac{N\pi \cdot BORE \cdot S_{rat}}{30} \tag{6}$$

where S_{rat} is the Woschni swirl ratio.

Preservation of the mass, energy and the sum of forces resulting from the pressure in pipes are modelled through the equation of continuity, moment and energy preservation. The collectors are based on a zero-dimensional calculation which, instead of the variable of length, operates with values of pressure, temperature, mass and volume. Friction is calculated with the aid of Howard Barner Moss model [11] which is applied exclusively in spark ignition (SI) engines. From operating parameters lambda was set to 0.9 and throttle fully opened. The cylinder geometry was known through geometrical parameters. The geometry of pipe, volumes and valve was estimated. The throttle diameter and flow coefficient were tuned together with flow coefficients from intake and exhaust ports to get the required filling for torque build up. Since no indication data was available, the Woschni and combustion parameters were kept to default values typical for gasoline engines.

As it can be observed in Figure 5, the peak model power corresponds to the maximum power of the real-life engine, amounting to 160 kW. The brake medium effective pressure (BMEP) is also real, as is the brake specific fuel consumption (BSFC). Information on the real engine's torque is not available. Simulations have been carried out at full load with the engine speed ranging from 1000 to 5000 rpm. The local peak occurs due to pressure pulsations in the intake runners. The pulsation creates pressure increase at a specific pressure pulsation frequency which is defined by pipe length intake manifold volume size. This results in the increase in delivery ratio at the region of 3500 rpm for this case.

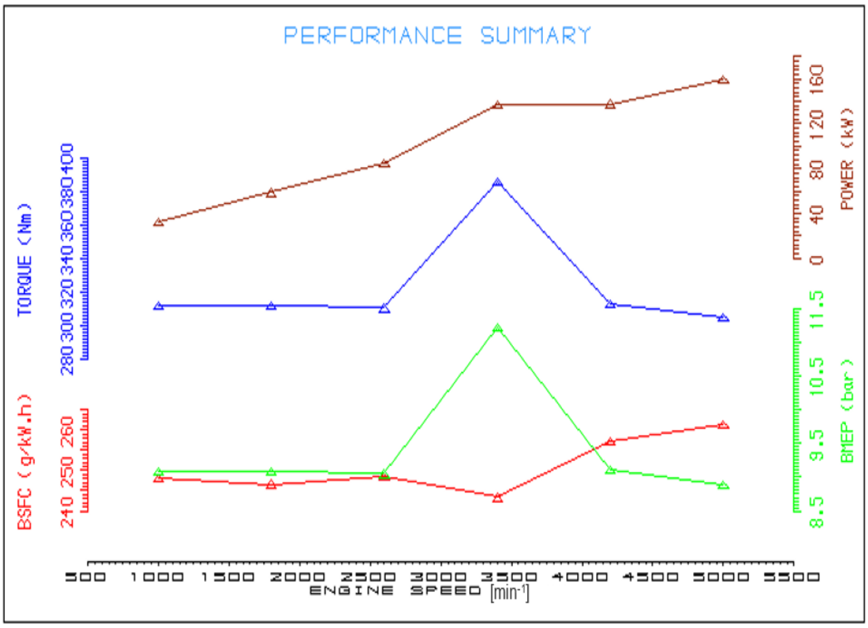

Fig. 5. Simulation results of the four stroke high speed 4.3l engine model

4. Concept validation

In standard turbochargers the turbine part is designed to meet the power required in the compression part of the turbocharger with the least possible impact of the backpressure at the exhaust. The energy potential that can be delivered to the turbine remains unused due to low expansion features of the turbine, defined by the design of the bypass or exhaust valves, aimed at protection against excessive compression pressure at the inlet part of the engine (*wastegate*, *blowoff*). By separating the turbine from the compression part and by connecting it to the generator, it is now possible to use, in a more efficient way, the energy potential of the turbines having even higher compression ratios. As the turbine gets larger, compared to conventional sizes, the influence of the backpressure in the exhaust line gets larger as well, and this causes engine's throttle, i.e. loss of power. The power loss can be reduced through the optimisation of turbine parameters and by mounting an adequate compressor. A conceptual description of this solution will be presented afterwards.

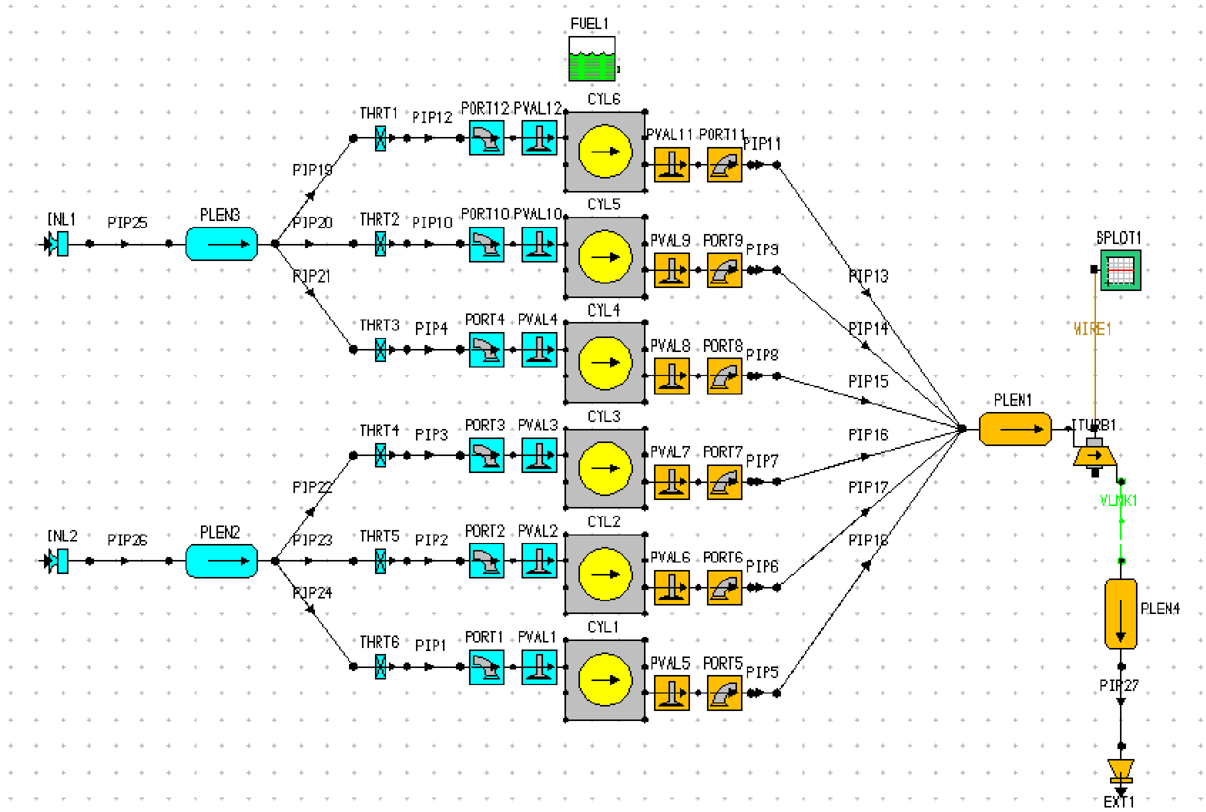

Fig. 6. Engine model with an independent turbine

Figure 6 presents the basic model for a naturally aspirated engine fitted with an available turbine connected to the exhaust line and a 6-litre exhaust manifold. Figure 7 features the turbine efficiency map with regard to the mass flows of exhaust gases and the corrected speed. Since no hotbench data was available the turbine map was taken from the existing library and scaled so that the surgeline mass flow value under map defined expansion ratios matches the cylinders filling demand at the engine full load operation, avoiding maximum torque limits.

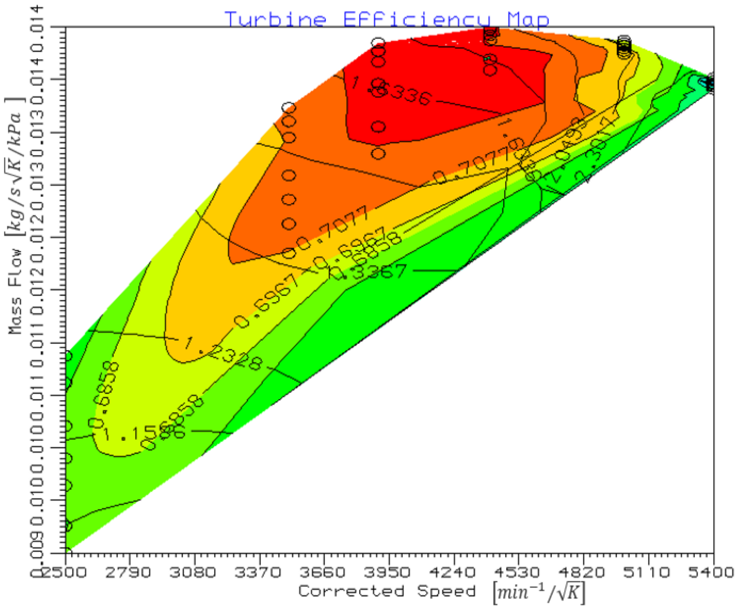

Fig. 7. Turbine efficiency map vs mass flow

The x axis shows the corrected speed n_{cor} that indicates the ratio of the turbine wheel speed and the root of the turbine's inlet temperature [10]:

$$n_{cor} = \frac{n_{tur}}{\sqrt{T_{inl}}} \tag{7}$$

where n_{tur} is the turbine wheel speed and T_{inl} is the temperature of exhaust gases at the turbine's inlet.

The y axis shows the corrected mass flow through the turbine [10], equal to:

$$\dot{m}_{tur} = \frac{\dot{m}_{tt} \cdot \sqrt{T_{inl}}}{p_{inl\_abs}} \tag{8}$$

where $\dot{m}_{tt}$ is the theoretical mass flow through the turbine, while p_{inl_abs} is the absolute pressure at the turbine's inlet.

Figure 8 features the turbine efficiency map with regard to pressure ratios and mass flows of exhaust gases.

The pressure ratio [11] is defined as:

$$PR = \frac{p_{inl\_abs}}{p_{out\_abs}} \tag{9}$$

where p_{out_abs} is the absolute pressure at the outlet of the turbine.

The overall efficiency of the turbine [5] is calculated through the equation:

$$\eta = \frac{\Delta h_{u\_i}}{\Delta h_{PR}} \tag{10}$$

where Δh_{u_i} is the real enthalpy drop across the turbine, while Δh_{PR} is the isentropic enthalpy drop across the turbine, directly proportional to the pressure ratio.

The following paragraphs describe the performed simulation of the operation of the engine fitted with a turbine that provides power for driving generators.

The brake power and fuel consumption compared to an engine without a turbine is shown in Figure 8.

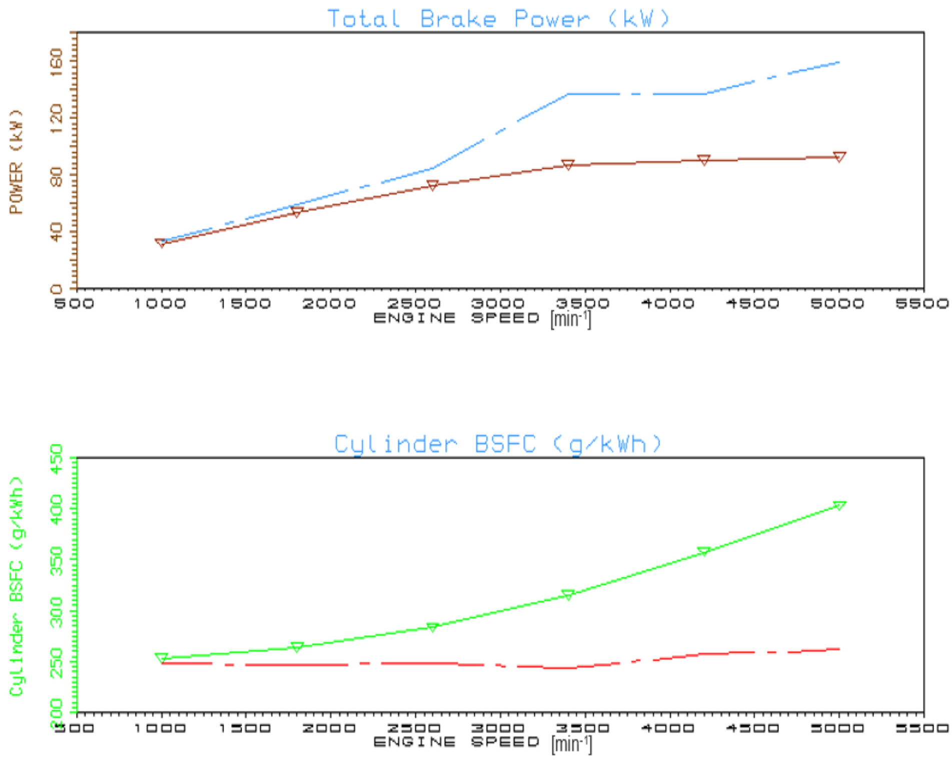

Fig. 8. Brake power and specific fuel consumption comparison

The brown and green colours present the achieved brake power and fuel consumption in the engine fitted with a turbine, whereas the results of the conventional engine are shown in blue and red colours. It can be noted that the engine power decreases due to throttling caused by the turbine, while the consumption increases considerably.

Considering the loss in the engine itself amounting to around 60 kW due to throttling and the significantly increased consumption, it can be concluded that fitting a turbine to the exhaust line is not an optimal solution, because of significant increase in specific consumption, reduced performance and the overall loss of around 30 kW in the engine-turbine system. Hence it is logical to increase the compression potential of the engine by providing a belt-driven compressor. The latter increases charging pressure, volumetric efficiency and overcomes additional backpressure caused by the turbine on the exhaust line.

5. Modelling of the TERS and the turbine optimisation

Mounting a compressor at the inlet part would increase the potential of the inlet mixture to the engine, which would reduce the throttling effect in the engine and increase the work in the turbine. The compressor is designed to enable the engine maintain power on the output shaft equal to the power in the standard naturally aspirated engine, with an increase in specific consumption kept as low as possible. In this way, the power achieved in the turbine would be added to the power on the shaft, which would make the system more cost-efficient and would considerably increase the overall system efficiency.

Figure 9 presents the model for an engine fitted with a turbine and an engine belt-driven compressor. The system also features a modelled charge air cooler.

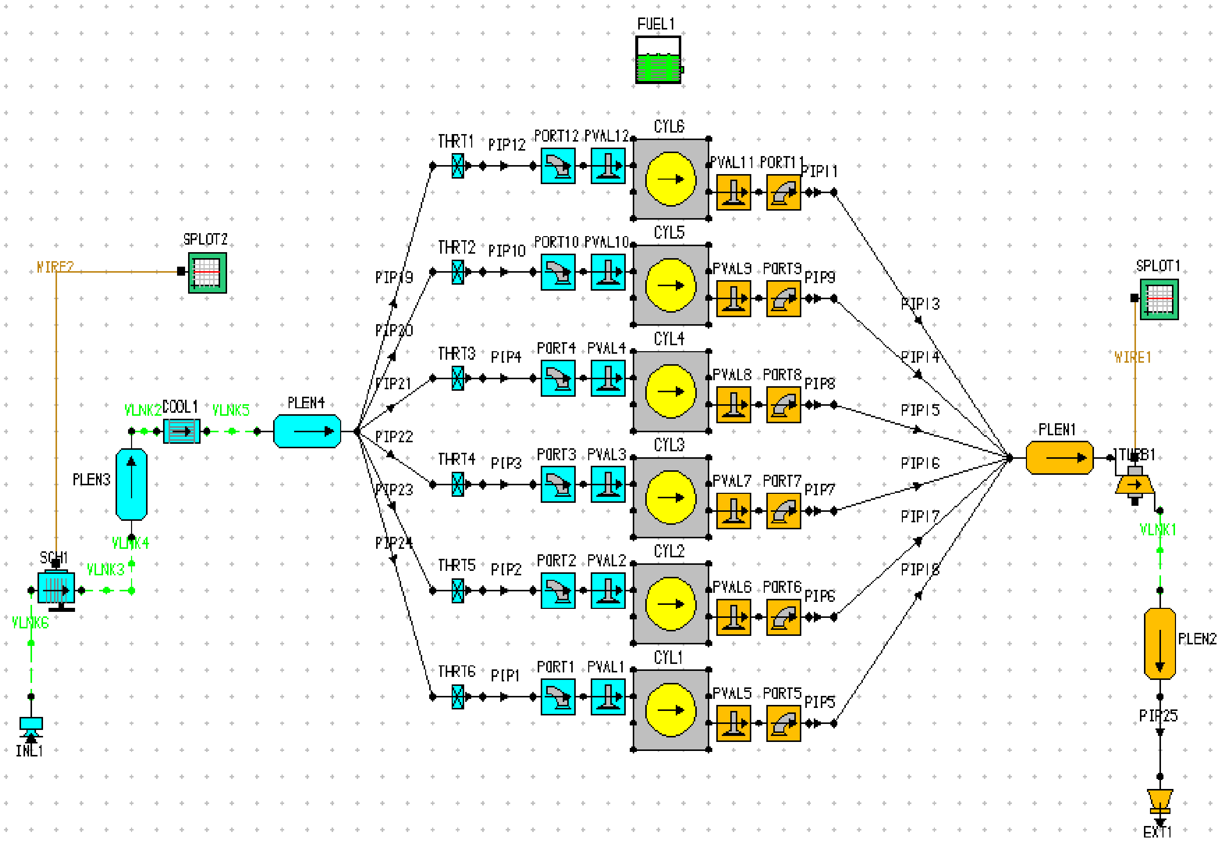

Fig. 9. Engine model with a compressor and a turbine

After performing simulations of the engine model with a compressor and a turbine, the results of the achieved power and consumption have been compared with the conventional engine, the engine fitted only with a turbine, and the engine with both the compressor and turbine at full load (Figure 10).

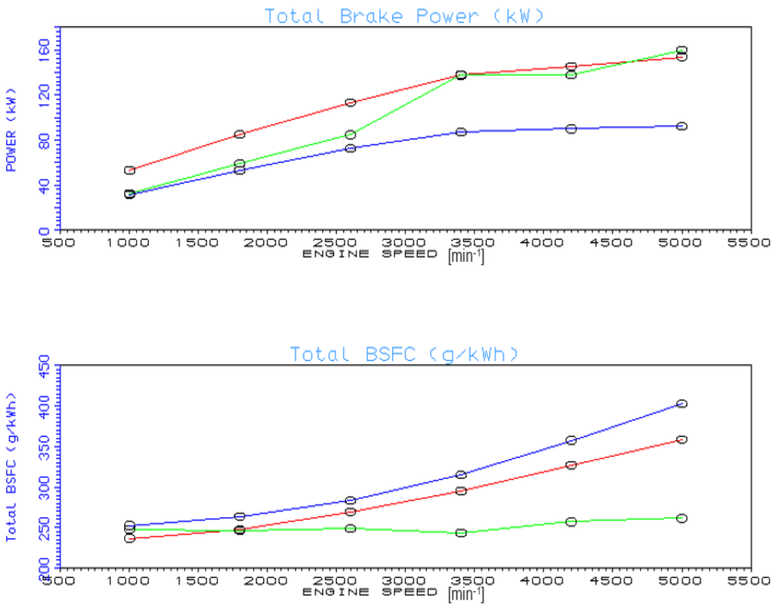

Fig. 10. Comparison of the three powertrain combinations

Green lines indicate the diagrams of power and consumption in a conventional engine; blue lines show these values in a turbine-engine; red lines show these values in an engine fitted with a compressor and a turbine. The diagram proves that the combination with a compressor and a turbine is optimal, given the fact that the power is maintained at higher loads and increased at lower loads, compared to the standard naturally aspirated engine. It is true that this combination involves an increased specific consumption, but the specific consumption calculation takes into account just the power on the outlet shaft. By increasing consumption by approximately 50 g/kWh, compared to the naturally aspirated engine, the initial power of the naturally aspirated engine is maintained, while the power in the turbine exceeds 50 kW. If the power in the turbine is included in the calculation of specific consumption, this results in the total specific consumption of 244 g/kWh which is lower than the specific consumption in the naturally aspirated engine. It can be concluded that the system fitted with the standalone compressor and turbine provides 50 kW more useful power while the specific consumption remains the same, which means that this system is more efficient.

The power achieved by the turbine exceeds 55 kW at 5000 rpm engine speed. This power would be otherwise released into the environment in its thermal and kinetic form. However, it is now possible to further use this power for battery charging or direct distribution to the consumers through electric motors.

In order to make the system more cost-effective, it is necessary to optimally use the work of the turbine and to minimise the effect of engine throttling, i.e. it is necessary to optimise the turbine operation parameters.

The first optimisation cycle consists of optimising the dimensions of the turbine's inlet and outlet gates with the purpose of achieving the least possible resistance and pressure variations. The objective function involves the minimum deviation of the power curve from the previous simulation of the engine with the separate turbine and compressor (Figure 11, red curve indicating power). The first optimisation variable is the turbine's inlet diameter with limited or boundary values, i.e. the minimum diameter being 30 mm, maximum diameter being 90 mm, and inspection step being 20 mm. The second optimisation variable is the turbine's outlet diameter with limited or boundary values, i.e. the minimum diameter being 60 mm, maximum diameter being 120 mm, and inspection step being 20 mm.

Optimum results have been obtained after performing 16 cycles of 2D optimisation. The optimisation implies pairing up each of the given variables in every possible combination. A simulation of the engine at full load across the engine speed range is conducted for each of the combinations. The optimal results are shown in Figure 11.

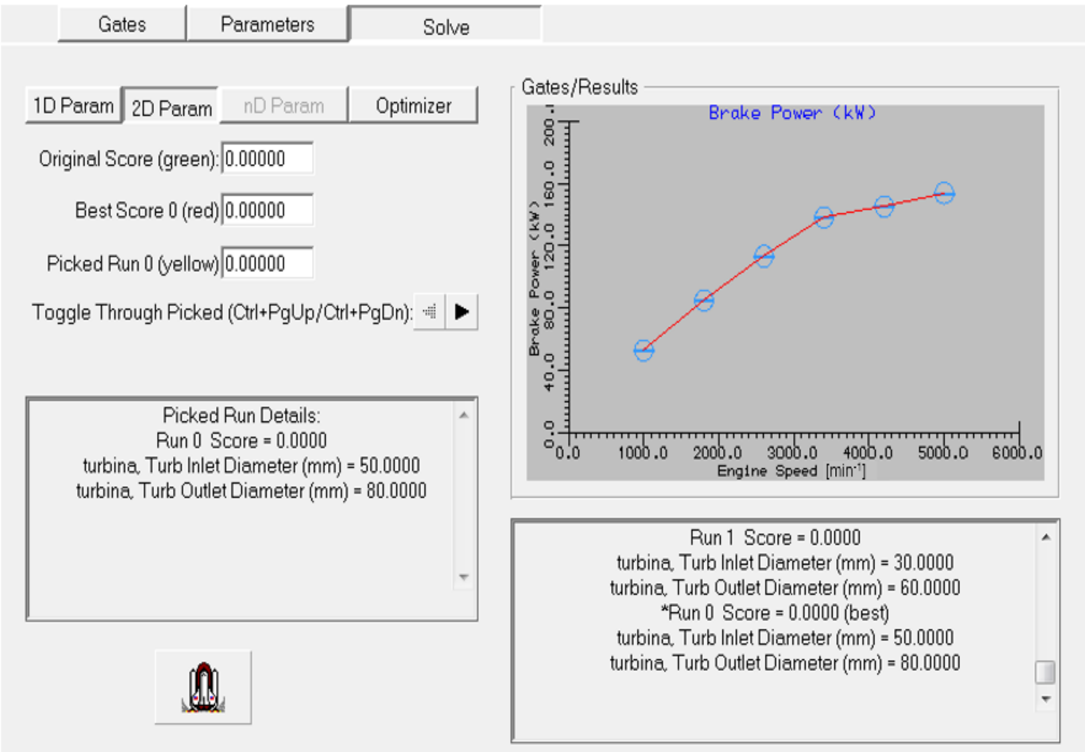

Fig. 11. Results of the optimisation

The optimisation results produce a power curve that indicates the least deviation of the engine power from the objective function. The optimal results include the turbine inlet diameter of 50 mm and the outlet diameter of 80 mm.

The optimised values of the turbine inlet and outlet gates produce the peak power of 59 kW in the turbine in relation to the engine speed (Figure 12).

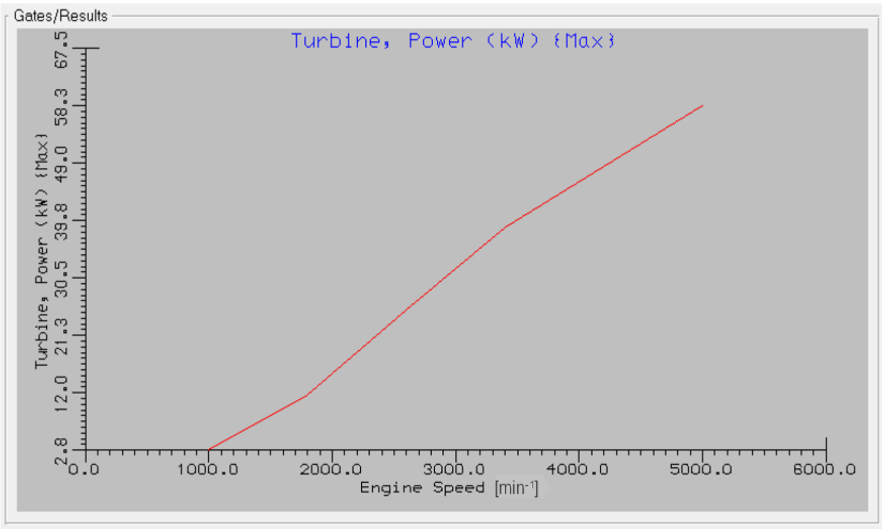

Fig. 12. Peak turbine power vs engine speed

Definition of operating turbine parameters in reference to the engine speed provides an insight into the relation of all operating parameters of the turbine, which has to be taken into consideration when selecting or designing the turbine.

The isentropic efficiency in relation to the engine speed at full load is shown in Figure 13.

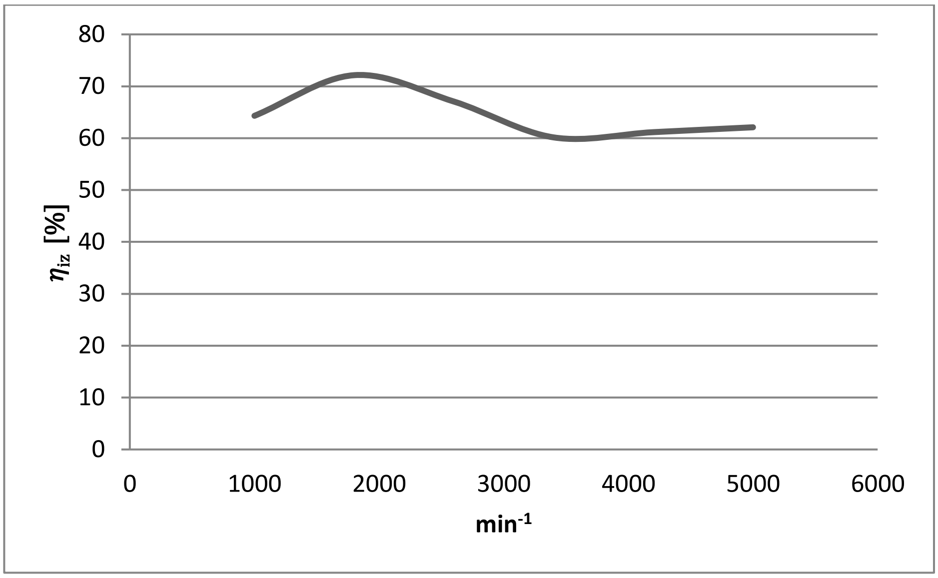

Fig. 13. Turbine isentropic efficiency vs engine speed at full load

The power at the outlet turbine shaft in reference to the engine speed at full load is shown in Figure 14.

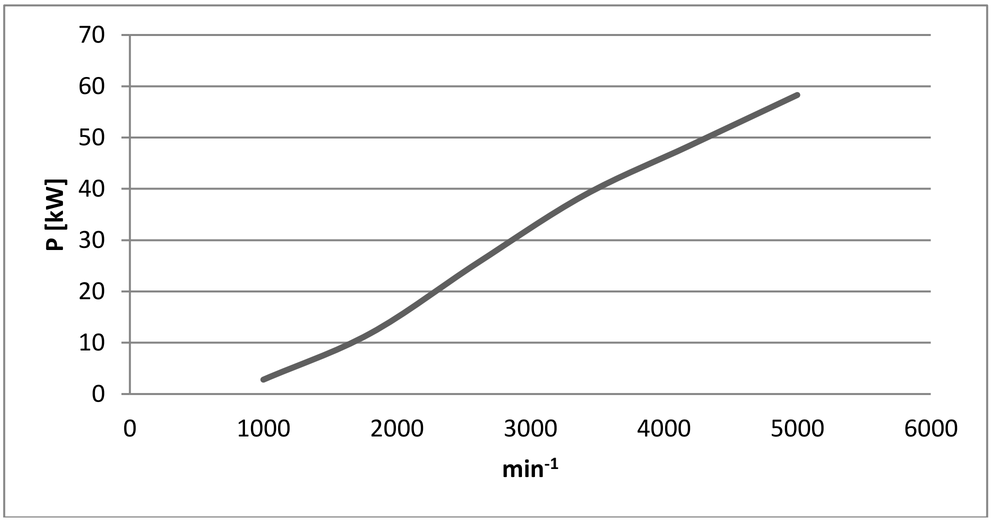

Fig. 14. Turbine power vs engine speed at full load

6. Conclusion

The innovative turbine-engine recuperation concept (TERS) achieves higher efficiency of the propulsion system and lower harmful emissions. Simulations and optimisation of the engine and turbine models were performed, indicating that the increase in efficiency of the hybrid system implies the reduced specific consumption, without compromising the consumers' need for energy. The increased recuperation of energy from exhaust gases is used for charging batteries or supplying onboard consumers. The electric power stored in batteries is intended for electric propulsion in coastal waters where an internal combustion engine runs at low loads, hence outside optimal range, and where stricter international regulations on exhaust emissions are applied. The innovative hybrid concept of TERS system will be a preferable solution for future marine propulsion systems.

Acknowledgements

We would like to extend our sincere gratitude and appreciation to Lotus Engineering Software Company for using their software package and their support in the development of this innovative model.

References:

[1] Fraser, H., Blaxill, H., Lumsden, G., Bassett, M.: "Challenges for increased efficiency through gasoline engine downsizing", SAE Int. J. Engines 2 (2001), pp. 991-1008. https://doi.org/10.4271/2009-01-1053.

[2] Bandel, W., Fraidl, G., Kapus, P., Sikinger, H. et al.: "The Turbocharged GDI Engine: Boosted Synergies for High Fuel Economy Plus Ultra-Low Emission", SAE Technical Paper (2006), 2006-01-1266, doi: 10.4271/2006-01-1266. https://doi.org/10.4271/2006-01-1266.

[3] Tóth-Nagy, C., Investigation and Simulation of the Planetary Combination Hybrid Electric Vehicle, Department of Mechanical and Aerospace Engineering Morgantown, West Virginia, 2000.

[4] Grljušić, M., Medica, V., Radica, G.: "Calculation of Efficiencies of a Ship Power Plant Operating with Waste Heat Recovery through Combined Heat and Power Production", Energies, 2015, 8, pp. 4273-4299. https://doi.org/10.3390/en8054273.

[5] Grljušić, M., Medica, V., Račić, N.: "Thermodynamic Analysis of a Ship Power Plant Operating with Waste Heat Recovery through Combined Heat and Power Production", Energies, 2014, 7, pp. 7368-7394. https://doi.org/10.3390/en7117368.

[6] Radica G., Antonić, R., Račić, N.: "Engine Working Cycle Analysis for Diagnostic and Optimisation Purposes", Brodogradnja, 2009, 4, 621.436:62-9.

[7] Fu, J., Tang, Q., Liu, J., Deng, B., Yang, J., Feng, R.,: "A combined air cycle used for IC engine supercharging based on waste heat recovery", Energy Conversion and Management, (2014), 87, pp. 86-95. https://doi.org/10.1016/j.enconman.2014.06.097.

[8] Mardi, M. K., Khalilarya, S., Nemati, A.: "A numerical investigation on the influence of EGR in a supercharged SI engine fueled with gasoline and alternative fuels", Energy Conversion and Management, (2014), 83, pp. 260-269. https://doi.org/10.1016/j.enconman.2014.03.031.

[9] Carlucci, A., P., Ficarella, A., Trullo, G.: "Performance optimization of a Two-Stroke supercharged diesel engine for aircraft propulsion", Energy Conversion and Management, (2016), 122, pp. 279-289.

[10] Lotus user manual, Lotus, 2012. ttps://doi.org/10.1016/j.enconman.2016.05.077.

[11] Barness-Moss, H. W.: "A Designers Viewpoint", International Mechanical Engineering, C343/73.

List of symbols and abbreviations

A, B, C and D	Woschni coefficients
A and M	coefficient of the Vibe function
AC/DC	converter of alternating current into direct current
DC/AC	converter of direct current into alternating current
D_{cyl}	cylinder bore
h	heat transfer coefficient
m_{frac}	fraction of burned fuel mass
$\dot{m}_{tur}$	corrected mass flow through the turbine
$\dot{m}_{tt}$	theoretical mass flow through the turbine
n_{tur}	turbine wheel speed
N	engine speed
n_{cor}	corrected speed
p	cylinder pressure

p_{inl_abs}	absolute pressure at the turbine inlet
p_{motor}	motoring pressure
p_{out_abs}	absolute pressure at the turbine outlet
p_{SOC}	pressure at the start of combustion
PR	planetary gear reducer
R	gear reducer
S_{rat}	Woschni swirl ratio
T	cylinder temperature
T	consumer
T_{inl}	exhaust gas temperature at the turbine inlet
T_{SOC}	temperature at the start of combustion
$\bar{U}_{swirl}$	mean swirl speed
$\bar{U}_{piston}$	mean piston speed
V	volume in the cylinder
V_{SOC}	volume at the start of combustion

Greek letters

Δh_{u_i}	real enthalpy drop across the turbine
Δh_{PR}	isentropic enthalpy drop across the turbine, directly proportional to the pressure ratio
η	overall turbine efficiency
θ	crankshaft angle
θ_b	combustion period

Submitted: 03.02.2017.

Accepted: 08.05.2017.

Mag. Ing. Mech. Nikola Matulić, Ph. D. candidate, nimatulic@gmail.com
Ph. D. Gojmir Radica, professor, gojmir.radica@fesb.hr
Faculty of electrical engineering, mechanical engineering and naval architecture
University of Split, Ruđera Boškovića 32, 21000 Split
Ph. D. Nikola Račić, associate professor, nikola.racic@pfst.hr
Faculty of Maritime Studies, University of Split, Ruđera Boškovića 37, 21000 Split